Volume 60
Number 52
4 July 2024
Pages 6571–6692

ChemComm

Chemical Communications

rsc.li/chemcomm

ISSN 1359-7345

ROYAL SOCIETY OF CHEMISTRY

COMMUNICATION

Takeharu Haino *et al.*

Selective encapsulation of carboxylic acid dimers within a size-regulable resorcinarene-based hemicarcerand

60 YEARS ANNIVERSARY

ChemComm

COMMUNICATION

View Article Online
View Journal | View Issue

Cite this: *Chem. Commun.*, 2024, **60**, 6603

Received 11th February 2024,
Accepted 27th May 2024

DOI: 10.1039/d4cc00699b

rsc.li/chemcomm

Selective encapsulation of carboxylic acid dimers within a size-regulable resorcinarene-based hemicarcerand†

Kentaro Harada,[a] Yudai Ono,[ab] Ryo Sekiya[a] and Takeharu Haino*[ab]

A cavity within a resorcinarene-based hemicarcerand was contracted and expanded through conformational changes induced by the complexation and decomplexation, allowing self-sorting of homo- and heterodimeric carboxylic acid pairs.

Allosteric regulation is crucial for controlling metabolic pathways, which modify the activity of proteins in response to effector binding.[1–5] For example, calmodulin exhibits allosteric behavior.[6] When a calcium ion binds to the remote site of calmodulin, the structure of the hydrophobic binding pocket is deformed. This process allows for the selective binding of target proteins, such as myosin light-chain kinase. Abiotic molecular capsules with large internal cavities that can accommodate guests with large molecular dimensions have been developed to mimic the allosteric regulation of proteins.[7–25] Light,[26–31] metals,[32–35] pH,[36–39] and anions[40,41] act as effectors that activate or deactivate binding sites, which drive the uptake or release of guest molecules in an allosteric manner. Abiotic allosteric molecules can be applied in many potential applications, including drug delivery,[42,43] catalysis,[44,45] and sensing.[46,47] Many efforts have been devoted to developing size-adjustable abiotic capsules in which guest encapsulation is switchable however, developing an artificial molecular cavity that can self-sort specific guest pairs among several possible pairs has been a great scientific challenge.[48–53]

Hemicarcerand **1** is a unique molecular container that possesses an internal cavity (Fig. 1a). This cavity can be contracted and expanded by metal complexation and decomplexation, respectively, which is accompanied by switchable molecular recognition.[54,55] Herein, we report the development of homo and heterodimeric carboxylic acid pairs with self-sorting behaviors inside the cavity of **1**. Carboxylic acids are known to dimerize in lipophilic solvents,[56,57] and mixtures of multiple carboxylic acids generate homo and heterodimeric pairs according to a statistical distribution. Thus, it is generally difficult to selectively obtain a desired dimeric pair. The cavity of **1** and the Ag-coordinated hemicarcerand (**1Ag**) provided expanded and contracted environments, respectively, in which homo (**G2a**·**G2a**) or heterodimeric (**G1a**·**G2a**) pairs were selectively formed in a self-sorting manner (Fig. 1b). The selective encapsulation of the dimeric carboxylic acid pairs was reversibly regulated upon the addition and removal of Ag^+ cations.

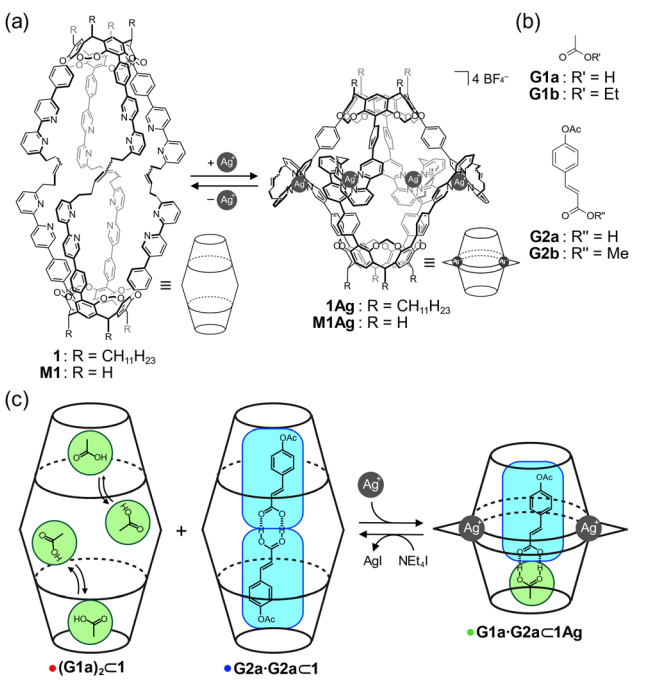

Fig. 1 (a) Molecular structures of **1** and **1Ag** and those of **M1** and **M1Ag** for DFT calculations. (b) Guests **G1a–b** and **G2a–b**. (c) Schematic representation showing the self-sorting behavior of homo and heterodimeric carboxylic acid pairs.

[a] *Department of Chemistry, Graduate School of Advanced Science and Engineering Hiroshima University, 1-3-1 Kagamiyama, Higashi-Hiroshima, Hiroshima, 739-8526, Japan. E-mail: haino@hiroshima-u.ac.jp*

[b] *International Institute for Sustainability with Knotted Chiral Meta Matter (WPI-SKCM²), Hiroshima University, 2-313 Kagamiyama, Higashi-Hiroshima, Hiroshima, 739-0046, Japan*

† Electronic supplementary information (ESI) available. See DOI: https://doi.org/10.1039/d4cc00699b

Reversible contraction and expansion of the cavity was achieved by the interconversion between **1** and **1Ag**. The aromatic proton signals of **1** were assigned entirely in chloroform-d_1 (Fig. 2a). The addition of two equivalents of $AgBF_4$ to a solution of **1** caused downfield shifts in the pyridyl protons H_a–H_e as a result of the reduced electron density of the bipyridyl arms due to Ag–N coordination. In contrast, the pyridyl proton H_f, which was located within the shielding region of the neighboring bipyridyl arm in the tetrahedral coordination geometry, exhibited an upfield shift of 0.50 ppm. The eight arms showed equivalent signals, indicative of the D_4 symmetry on the NMR time scale. The electrospray ionization mass spectrum showed ion peaks corresponding to $[\mathbf{1}{+}Ag_4]^{4+}$ and $[\mathbf{1}{+}Ag_4(BF_4)]^{3+}$. The isotope pattern of $[\mathbf{1}{+}Ag_4(BF_4)]^{3+}$ corresponded well with the simulated result (Fig. S3 in ESI†).

The host–guest complexation of **1** was evaluated by ^{1}H NMR spectroscopy (Fig. 3). A mixture of **1** and **G1a** generated methyl protons of bound **G1a** at approximately $\delta = -1.6$ ppm (Fig. 3a), which led to exchange cross peaks between the bound and free **G1a** (Fig. S9 in ESI†). The large upfield shifts indicated that **G1a** was encapsulated in **1**. The signals consisted of broad and weak sharp signals. As the bipyridyl arms function as Lewis bases, **G1a** can anchor to the bipyridyl arms. Thus, the methyl protons of bound guests show sharp signals due to their methyl groups at the bottom of the capsules, which form C–H/π interactions.[54,58] Hence, the sharp signal was tentatively assigned as **G1a** at the bottom of **1**, and the broad signal originated from **G1a** anchoring to the bipyridyl arms. The integration of the signals indicated that two molecules of **G1a** were encapsulated in **1** (Fig. S4 in ESI†). This host–guest complex was named $(\mathbf{G1a})_2{\subset}\mathbf{1}$.

A mixture of **1** and **G2a** generated only a sharp signal corresponding to the methyl protons of **G2a** at $\delta = -1.27$ ppm (Fig. 3b). Based on the signal intensity, the host–guest ratio was determined to be 1 : 2 (Fig. S12 in the ESI†). NOEs were observed between the methyl protons of **G2a** and the methylene bridges of **1** (Fig. S11 in ESI†), indicating that the methyl group was located at the bottom of **1**, resulting in the C–H/π interactions. Hence, the carboxy group was pointed to the center of the cavity, indicating that the hydrogen-bonded dimer was formed in the host–guest complex **G2a**·**G2a**⊂**1**.

A control experiment showed that the COOH group is required for the host–guest complexation of **1** when esters

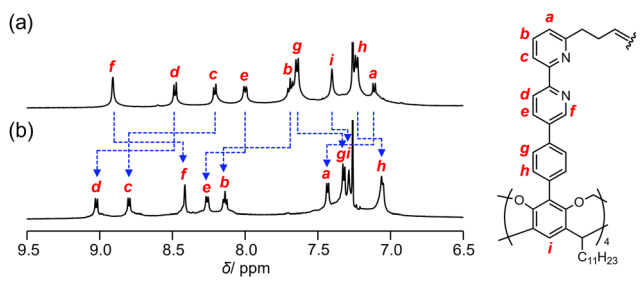

Fig. 2 Selected region of the ^{1}H NMR spectra (500 MHz, chloroform-d_1, 298 K) of (a) **1** and (b) **1Ag**.

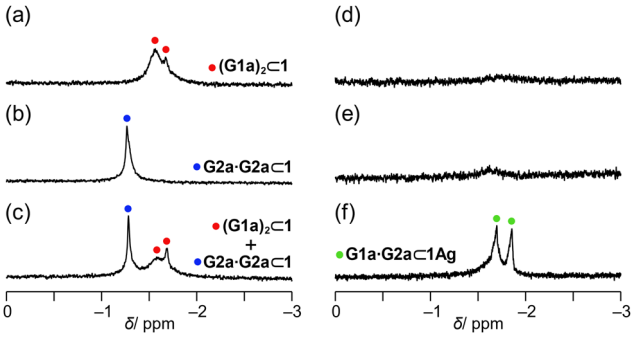

Fig. 3 Selected region of the ^{1}H NMR spectra (500 MHz, chloroform-d_1, 223 K) of the mixture of capsule **1** (1.5 mM) and (a) **G1a** (15 mM), (b) **G2a** (15 mM), and (c) **G1a** (15 mM) and **G2a** (15 mM) and the mixture of capsule **1Ag** (1.5 mM) and (d) **G1a** (15 mM), (e) **G2a** (15 mM), and (f) **G1a** (15 mM) and **G2a** (15 mM).

G1b and **G2b** were employed. ^{1}H NMR spectra showed no signals assignable to bound **G1b** and **G2b** (Fig. S13 in ESI†). Because **1** can adjust its cavity for the bound guests,[54] the longer size of **G2b** than **G2a** would not be responsible for the no host–guest complexation. Further, in THF-d_8 **G2a** was not trapped in **1** (Fig. S23 in ESI†). THF functions as a hydrogen bond acceptor. Thus, the hydrogen-bonded dimeric pair of **G2a** is weakened by the competitive solvation, which most likely interferes with host–guest complexation in THF-d_8, although the possibility of the encapsulation of THF in **1** instead of **G2a** cannot be ruled out. In view of these facts, the hydrogen-bonded dimeric form of **G2a** is crucial for host–guest complexation.

When **G1a** and **G2a** were mixed with **1**, two sets of signals appeared, which were assignable to $(\mathbf{G1a})_2{\subset}\mathbf{1}$ and **G2a**·**G2a**⊂**1** (Fig. 3c). The other signals of bound **G2a**·**G2a** resonated at the same chemical shifts as those of **G2a**·**G2a**⊂**1** alone (Fig. S4 in ESI†). When the heterodimeric form was organized, the methyl protons of **G1a** and **G2a** were expected to generate a 1 : 1 signal ratio, as in the case of **1Ag** (see below). However, these signals were not detected. These observations rationalize that the homodimeric form of **G2a** or two molecules of **G1a** were selectively encapsulated in **1**.

1Ag showed a distinct selectivity. Although a mixture of **1Ag** with **G1a** or **G2a** generated very weak signals (Fig. 3d and e), a mixture of **1Ag** with **G1a** and **G2a** generated methyl protons of **G2a** and **G1a** with a 1 : 1 signal intensity at $\delta = -1.69$ ppm and -1.86 ppm, respectively. Exchange peaks were observed between bound and unbound **G1a** and **G2a** (Fig. 4a). The methyl protons of bound **G1a** and **G2a** generated NOE correlations with the bridge methylene signals H_j at 223 K (Fig. 4b), revealing that the methyl groups of **G1a** and **G2a** were located at the bottom of **1Ag**; thus, the carboxy groups of these compounds faced each other in the cavity. Accordingly, **G1a**·**G2a** was likely to be organized in **1Ag**. The host–guest complexation was supported by ^{1}H DOSY, wherein the diffusion coefficients of bound **G1a** and **G2a** were consistent with that of **1Ag** (Fig. 4c).

To evaluate the structural feasibility of the host–guest complexes, density functional theory calculations were carried out

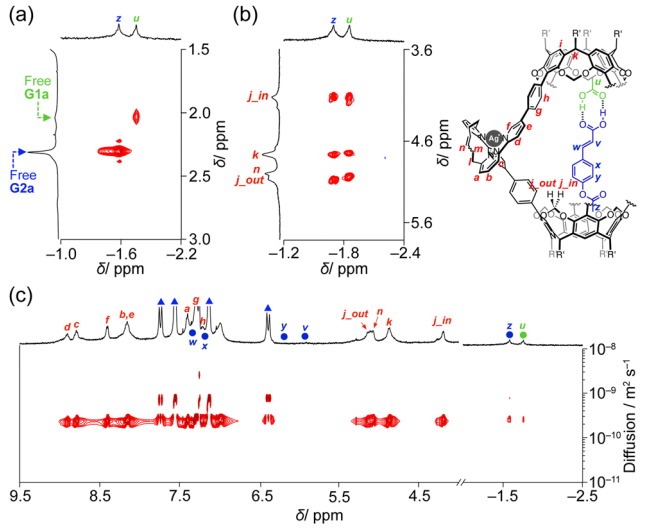

Fig. 4 (a) and (b) Selected region of the 2D NOESY spectra (500 MHz, chloroform-d_1) of the mixture of **1Ag** (1.5 mM), **G1a** (15 mM) and **G2a** (15 mM) at (a) 298 K and (b) 223 K. (c) DOSY spectra (500 MHz, chloroform-d_1, 298 K) of the mixture of **1Ag** (1.5 mM), **G1a** (15 mM) and **G2a** (15 mM). The blue and green filled circles denote bound **G2a** and **G1a**, respectively, and the blue filled triangles denote unbound **G2a**.

using **M1** and **M1Ag**, in which the long alkyl chains on the lower rim were replaced with hydrogen atoms.[59] The optimized structures of **G1a**·**G2a**⊂**M1** (Fig. S22a in ESI†) and **G2a**·**G2a**⊂**M1** (Fig. 5a) suggested that the homodimer fit well within **M1**. For **G1a**·**G2a**⊂**M1**, the cavity must be squeezed to fit the heterodimer, which involves folding the alkyl chains that connect two cavitands; these movements cause an energetic penalty, which should contribute to the selective organization of **G2a**·**G2a**⊂**1** over **G1a**·**G2a**⊂**1**.

Although the homodimer **G2a**·**G2a** could not fit within the interior of **1Ag** (Fig. 5b), which has a cavity height of 14.5 Å, the heterodimer **G1a**·**G2a** was complementary to the interior of **1Ag**; this complementarity explains the selective formation of **G1a**·**G2a**⊂**1Ag**.

The regulatable structural features of **1** were studied in solution. $AgBF_4$ was added to a solution of **1** in chloroform-d_1,

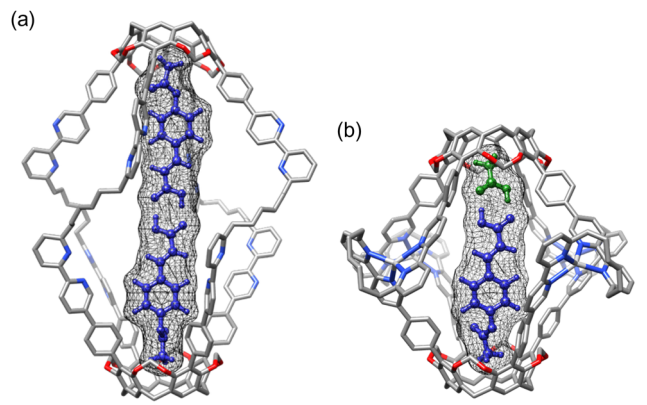

Fig. 5 Optimized structures of (a) **G2a**·**G2a**⊂**M1** and (b) **G1a**·**G2a**⊂**M1Ag** at the B3LYP/6-31G(d) and B3LYP/6-31G(d)+LanL2DZ levels. Color scheme: gray (carbon), white (hydrogen), blue (nitrogen), red (oxygen), and pale gray (silver).

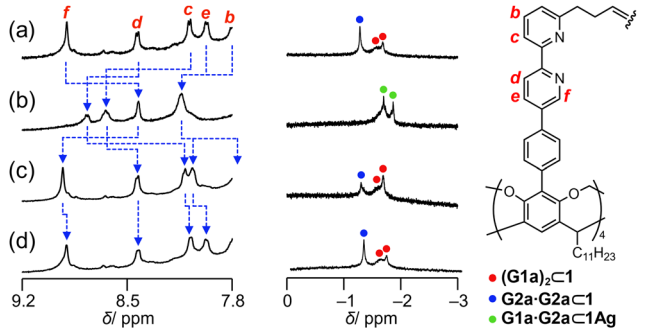

Fig. 6 Selected region of the ^{1}H NMR spectra (500 MHz, chloroform-d_1, 223 K) of (a) a mixture of **G1a** (10 mM), **G2a** (10 mM), and **1** (1.0 mM), (b) after four equivalents of $AgBF_4$ were added in acetonitrile-d_3 (60 μL) to the mixture, (c) after 8 equivalents of tetraethylammonium iodide in chloroform-d_1 (40 μL) were added to the solution, and (d) after removal of the solvents and dissolution of the resulting solid in chloroform-d_1.

resulting in **1Ag**. Then, tetraethylammonium iodide (NEt_4I) was added to expel the Ag^+ cations from **1Ag** as silver iodide (Fig. S18 in the ESI†). This structural interconversion was performed to induce *in situ* pair exchange between the homo and heterodimeric forms. Fig. 6 shows the change in the signals of the methyl groups of bound **G1a** and **G2a**. The mixture of **1** and the guests showed signals corresponding to bound **G1a** and **G2a**·**G2a** (Fig. 6a). When four equivalents of $AgBF_4$ in acetonitrile-d_3 were added to the solution, two signals assignable to **G1a**·**G2a**⊂**1Ag** were observed (Fig. 6b). The decomplexation of **1Ag** with 8 equivalents of NEt_4I resulted in the conversion of **G1a**·**G2a**⊂**1Ag** to (**G1a**)$_2$⊂**1** and **G2a**·**G2a**⊂**1** (Fig. 6c), although the presence of coexisting acetonitrile-d_3 influenced their relative ratio. The original spectrum was recovered by the concentration of the solvents and then adding chloroform-d_1 (Fig. 6d). The changes in chemical shifts of the bipyridyl arms (the blue broken lines in Fig. 6a–d) confirmed that the cavity expanded and contracted. A series of experiments showed that bound carboxylic acids underwent pair exchanges *in situ* by complexation and decomplexation.

In conclusion, resorcinarene-based hemicarcerand **1**, which possesses bipyridyl arms, self-sorted the carboxylic acid pairs by contracting and expanding the cavity through the complexation and decomplexation of Ag^+ cations in solution. In the expanded form, the homodimeric form of **G2a** or two molecules of **G1a** were encapsulated, while the heterodimeric forms of **G1a** and **G2a** were selectively organized in **1Ag**.

This work was supported by JSPS KAKENHI, Grants-in-Aid for Transformative Research Areas, "Condensed Conjugation" Grant Number JP21H05491 and "Materials Science of Meso-Hierarchy" Grant Number JP23H04873, and Grants-in-Aid for Scientific Research (A) Grant Number JP21H04685. We are also grateful to the KEIRIN JKA, Grant Number 2023M-419. K. H. acknowledges the Grand-in-Aid for the JSPS KAKENHI, Grant number 21J22939.

Conflicts of interest

There are no conflicts to declare.

Notes and references

1 M. F. Perutz, *Nature*, 1970, **228**, 726–734.
2 C. M. Revankar, D. F. Cimino, L. A. Sklar, J. B. Arterburn and E. R. Prossnitz, *Science*, 2005, **307**, 1625–1630.
3 Y.-C. Tang, H.-C. Chang, A. Roeben, D. Wischnewski, N. Wischnewski, M. J. Kerner, F. U. Hartl and M. Hayer-Hartl, *Cell*, 2006, **125**, 903–914.
4 F. U. Hartl, A. Bracher and M. Hayer-Hartl, *Nature*, 2011, **475**, 324–332.
5 H. R. Saibil, W. A. Fenton, D. K. Clare and A. L. Horwich, *J. Mol. Biol.*, 2013, **425**, 1476–1487.
6 D. E. Clapham, *Cell*, 2007, **131**, 1047–1058.
7 J. Rebek, Jr., *Acc. Chem. Res.*, 1984, **17**, 258–264.
8 J.-M. Lehn, *Science*, 1985, **227**, 849–856.
9 S. K. Körner, F. C. Tucci, D. M. Rudkevich, T. Heinz and J. J. Rebek, *Chem. – Eur. J.*, 2000, **6**, 187–195.
10 J. J. Rebek, *Chem. Commun.*, 2000, 637–643, DOI: 10.1039/A910339M.
11 S. Shinkai, M. Ikeda, A. Sugasaki and M. Takeuchi, *Acc. Chem. Res.*, 2001, **34**, 494–503.
12 L. Kovbasyuk and R. Krämer, *Chem. Rev.*, 2004, **104**, 3161–3188.
13 N. C. Gianneschi, M. S. Masar and C. A. Mirkin, *Acc. Chem. Res.*, 2005, **38**, 825–837.
14 C. A. Hunter and H. L. Anderson, *Angew. Chem., Int. Ed.*, 2009, **48**, 7488–7499.
15 L. Adriaenssens and P. Ballester, *Chem. Soc. Rev.*, 2013, **42**, 3261–3277.
16 C. Kremer and A. Lützen, *Chem. – Eur. J.*, 2013, **19**, 6162–6196.
17 M. Raynal, P. Ballester, A. Vidal-Ferran and P. W. N. M. van Leeuwen, *Chem. Soc. Rev.*, 2014, **43**, 1734–1787.
18 A. M. Lifschitz, M. S. Rosen, C. M. McGuirk and C. A. Mirkin, *J. Am. Chem. Soc.*, 2015, **137**, 7252–7261.
19 A. Jana, S. Bähring, M. Ishida, S. Goeb, D. Canevet, M. Sallé, J. O. Jeppesen and J. L. Sessler, *Chem. Soc. Rev.*, 2018, **47**, 5614–5645.
20 J. S. Park and J. L. Sessler, *Acc. Chem. Res.*, 2018, **51**, 2400–2410.
21 R. Pinalli, A. Pedrini and E. Dalcanale, *Chem. Soc. Rev.*, 2018, **47**, 7006–7026.
22 I. A. Rather, S. A. Wagay, M. S. Hasnain and R. Ali, *RSC Adv.*, 2019, **9**, 38309–38344.
23 F. J. Rizzuto, L. K. S. von Krbek and J. R. Nitschke, *Nat. Rev. Chem.*, 2019, **3**, 204–222.
24 H.-J. Schneider, *Chem. Commun.*, 2019, **55**, 3433–3444.
25 E. Benchimol, B.-N. T. Nguyen, T. K. Ronson and J. R. Nitschke, *Chem. Soc. Rev.*, 2022, **51**, 5101–5135.
26 E. L. Piatnitski and K. D. Deshayes, *Angew. Chem., Int. Ed.*, 1998, **37**, 970–972.
27 M. Han, R. Michel, B. He, Y.-S. Chen, D. Stalke, M. John and G. H. Clever, *Angew. Chem., Int. Ed.*, 2013, **52**, 1319–1323.
28 F. A. Arroyave and P. Ballester, *J. Org. Chem.*, 2015, **80**, 10866–10873.
29 D.-H. Qu, Q.-C. Wang, Q.-W. Zhang, X. Ma and H. Tian, *Chem. Rev.*, 2015, **115**, 7543–7588.
30 X. Chi, W. Cen, J. A. Queenan, L. Long, V. M. Lynch, N. M. Khashab and J. L. Sessler, *J. Am. Chem. Soc.*, 2019, **141**, 6468–6472.
31 H. Wu, Y. Chen, L. Zhang, O. Anamimoghadam, D. Shen, Z. Liu, K. Cai, C. Pezzato, C. L. Stern, Y. Liu and J. F. Stoddart, *J. Am. Chem. Soc.*, 2019, **141**, 1280–1289.
32 P. N. W. Baxter, R. G. Khoury, J.-M. Lehn, G. Baum and D. Fenske, *Chem. – Eur. J.*, 2000, **6**, 4140–4148.
33 S. Hiraoka, K. Harano, M. Shiro and M. Shionoya, *Angew. Chem., Int. Ed.*, 2005, **44**, 2727–2731.
34 N. Kishi, M. Akita, M. Kamiya, S. Hayashi, H.-F. Hsu and M. Yoshizawa, *J. Am. Chem. Soc.*, 2013, **135**, 12976–12979.
35 D. Ogata and J. Yuasa, *Angew. Chem., Int. Ed.*, 2019, **58**, 18424–18428.
36 D. Ajami and J. Rebek, *J. Am. Chem. Soc.*, 2006, **128**, 15038–15039.
37 G. Cafeo, F. H. Kohnke, L. Valenti and A. J. P. White, *Chem. – Eur. J.*, 2008, **14**, 11593–11600.
38 G. Yu, X. Zhou, Z. Zhang, C. Han, Z. Mao, C. Gao and F. Huang, *J. Am. Chem. Soc.*, 2012, **134**, 19489–19497.
39 K. Kurihara, K. Yazaki, M. Akita and M. Yoshizawa, *Angew. Chem., Int. Ed.*, 2017, **56**, 11360–11364.
40 J. Mendez-Arroyo, J. Barroso-Flores, A. M. Lifschitz, A. A. Sarjeant, C. L. Stern and C. A. Mirkin, *J. Am. Chem. Soc.*, 2014, **136**, 10340–10348.
41 J. Mendez-Arroyo, A. I. d'Aquino, A. B. Chinen, Y. D. Manraj and C. A. Mirkin, *J. Am. Chem. Soc.*, 2017, **139**, 1368–1371.
42 C. L. D. Gibb and B. C. Gibb, *J. Am. Chem. Soc.*, 2004, **126**, 11408–11409.
43 M. Cacciarini, V. A. Azov, P. Seiler, H. Künzer and F. Diederich, *Chem. Commun.*, 2005, 5269–5271, DOI: 10.1039/B509990K.
44 R. J. Hooley and J. Rebek, *Chem. Biol.*, 2009, **16**, 255–264.
45 H. J. Yoon, J. Kuwabara, J.-H. Kim and C. A. Mirkin, *Science*, 2010, **330**, 66–69.
46 M. S. Masar, N. C. Gianneschi, C. G. Oliveri, C. L. Stern, S. T. Nguyen and C. A. Mirkin, *J. Am. Chem. Soc.*, 2007, **129**, 10149–10158.
47 H. J. Yoon and C. A. Mirkin, *J. Am. Chem. Soc.*, 2008, **130**, 11590–11591.
48 A. Shivanyuk and J. Rebek, *J. Am. Chem. Soc.*, 2002, **124**, 12074–12075.
49 O. Perraud, V. Robert, A. Martinez and J.-P. Dutasta, *Chem. – Eur. J.*, 2011, **17**, 4177–4182.
50 N. K. Beyeh, D. P. Weimann, L. Kaufmann, C. A. Schalley and K. Rissanen, *Chem. – Eur. J.*, 2012, **18**, 5552–5557.
51 T. Taira, D. Ajami and J. Rebek, Jr., *J. Am. Chem. Soc.*, 2012, **134**, 11971–11973.
52 A. Galán, V. Valderrey and P. Ballester, *Chem. Sci.*, 2015, **6**, 6325–6333.
53 S. H. A. M. Leenders, R. Becker, T. Kumpulainen, B. de Bruin, T. Sawada, T. Kato, M. Fujita and J. N. H. Reek, *Chem. – Eur. J.*, 2016, **22**, 15468–15474.
54 K. Harada, R. Sekiya and T. Haino, *Chem. – Eur. J.*, 2020, **26**, 5810–5817.
55 K. Harada, R. Sekiya and T. Haino, *J. Org. Chem.*, 2021, **86**, 4440–4447.
56 I. Kojima, M. Yoshida and M. Tanaka, *J. Inorg. Nucl. Chem.*, 1970, **32**, 987–995.
57 C. Colominas, J. Teixidó, J. Cemelí, F. J. Luque and M. Orozco, *J. Phys. Chem. B*, 1998, **102**, 2269–2276.
58 Y. Tsunoda, K. Fukuta, T. Imamura, R. Sekiya, T. Furuyama, N. Kobayashi and T. Haino, *Angew. Chem., Int. Ed.*, 2014, **53**, 7243–7247.
59 G. W. T. M. J. Frisch, H. B. Schlegel, G. E. Scuseria, M. A. Robb, J. R. Cheeseman, G. Scalmani, V. Barone, G. A. Petersson, H. Nakatsuji, X. Li, M. Caricato, A. V. Marenich, J. Bloino, B. G. Janesko, R. Gomperts, B. Mennucci, H. P. Hratchian, J. V. Ortiz, A. F. Izmaylov, J. L. Sonnenberg, D. Williams-Young, F. Ding, F. Lipparini, F. Egidi, J. Goings, B. Peng, A. Petrone, T. Henderson, D. Ranasinghe, V. G. Zakrzewski, J. Gao, N. Rega, G. Zheng, W. Liang, M. Hada, M. Ehara, K. Toyota, R. Fukuda, J. Hasegawa, M. Ishida, T. Nakajima, Y. Honda, O. Kitao, H. Nakai, T. Vreven, K. Throssell, J. A. Montgomery, Jr., J. E. Peralta, F. Ogliaro, M. J. Bearpark, J. J. Heyd, E. N. Brothers, K. N. Kudin, V. N. Staroverov, T. A. Keith, R. Kobayashi, J. Normand, K. Raghavachari, A. P. Rendell, J. C. Burant, S. S. Iyengar, J. Tomasi, M. Cossi, J. M. Millam, M. Klene, C. Adamo, R. Cammi, J. W. Ochterski, R. L. Martin, K. Morokuma, O. Farkas, J. B. Foresman and D. J. Fox, *Gaussian 16, Revision C.01*, Gaussian, Inc., Wallingford CT, 2016.